Asian Journal of Chemistry; Vol. 37, No. 11 (2025), 2826-2830
ASIAN JOURNAL OF CHEMISTRY
https://doi.org/10.14233/ajchem.2025.34650

Electrochemical Synthesis of Hybrid Bismuth Telluride Films with Graphene and Carbon Nanofibers for Enhanced Thermoelectric and Mechanical Performance

K.F. SAMAT[1,*], M.A.I.C. AZMAN[1], A.H.A. RASYED[1], M.A. ALIAS[1], N.A.L.H.A. RASHID[1], M.H. JALI[2], N.V. TOAN[3,4] and T. ONO[3]

[1]Faculty of Industrial and Manufacturing Technology and Engineering, Universiti Teknikal Malaysia Melaka, Durian Tunggal, Melaka, Malaysia
[2]Faculty of Electrical Technology and Engineering, Universiti Teknikal Malaysia Melaka, Durian Tunggal, Melaka, Malaysia
[3]Department of Mechanical Systems Engineering, Tohoku University, Aoba-ku Sendai, Japan
[4]FPT University, Ho Chi Minh City, Vietnam

*Corresponding author: E-mail: khairul.fadzli@utem.edu.my

Received: 7 August 2025 *Accepted*: 1 October 2025 *Published online*: 27 October 2025 AJC-22172

Thermoelectric materials offer a sustainable solution for converting waste heat into electricity, with bismuth telluride (Bi_2Te_3) being highly effective at room temperature. However, enhancing its electronic and mechanical properties in film form remains challenging. This study investigates the improvement of Bi_2Te_3 films through the inclusion of graphene and carbon nanofibers (CNFs). The nanocomposite films were synthesized *via* a three-electrode electrochemical deposition technique. Electrolytes were prepared using 0.75 g/L graphene nanoparticles and 1 g/L CNFs, subjected to rigorous stirring and intermittent sonication to ensure proper dispersion and suspension. Cyclic voltammetry guided deposition voltage selection. Graphene integration resulted in a 200% increase in electrical conductivity due to its superior conductive nature. CNFs enhanced mechanical strength, doubling hardness and increasing Young's modulus by 34%, attributed to the Hall-Petch effect and CNF reinforcement. This study highlights the potential of graphene and CNF integration to improve Bi_2Te_3-based thermoelectric materials for a range of waste heat recovery applications.

Keywords: Electrodeposition, Bismuth telluride, Thermoelectric, Nanocomposite film.

INTRODUCTION

The advancements in thermoelectric devices have garnered significant attention, largely due to the rapid progress in the micro-electromechanical systems (MEMS) for advanced sensors and transducers. The integration of thermoelectric devices with MEMS technology has catalyzed distinguished improvements in various applications such as localized thermal management, on-site temperature sensing and energy harvesting [1,2]. The thermoelectric generators (TEGs) emerge as a promising technology for energy harvesting, converting thermal energy directly into electrical energy *via* the Seebeck effect even in extreme temperature condition [3,4]. As global energy demands escalate and the urgency for sustainable solutions intensifies, TEGs present a viable approach to capturing waste heat from diverse sources, including industrial processes, automotive exhausts and ambient environmental heat. The efficiency of TEG devices is predominantly influenced by the thermoelectric materials employed. The overall performance of thermoelectric material can be analyzed by figure of merit (ZT) and a high ZT value involves a combination of a high Seebeck coefficient, high electrical conductivity and low thermal conductivity [5,6].

Nanocomposites play a pivotal role in enhancing thermoelectric performance, particularly by improving electronic properties. Moreover, the incorporation of nanocomposite strategies can lead to significant improvements in mechanical properties, contributing to the overall structural integrity and durability of thermoelectric materials [7]. Multi-wall carbon nanotubes (MWCNTs) inclusion in Bi_2Te_3 enhanced the composites' electrical conductivity, Seebeck coefficient and power factor, improving the thermoelectric figure of merit by 10% compared to pure Bi_2Te_3 [8]. Similarly, incorporating reduced graphene oxide (RGO) and carbon nitride into the Bi_2Te_3 matrix significantly improved thermoelectric performance, as proven by higher ZT values [9].

Carbon nanofibers (CNFs) and graphene in thermoelectric nanocomposites can enhance electrical conductivity, reduce thermal conductivity and improve mechanical properties [10].

Graphene increases the electrical conductivity of Bi_2Te_3 films by enhancing charge carrier mobility, while CNF improves the mechanical characteristics such as microhardness and Young's modulus [11]. This work investigates the effect of incorporating graphene and carbon nanofibers (CNFs) into Bi_2Te_3 films, with the objective of improving the micro-mechanical properties and thermoelectric performance of graphene-CNF/ Bi_2Te_3 nanocomposite films through their integration within the bismuth telluride matrix.

EXPERIMENTAL

The nanocomposite film was synthesized by a potentiostatic electrochemical deposition system with a three-electrode cell a room temperature. The electrochemical cell consists of a Pt strip as a counter electrode (CE), silver/silver chloride (Ag/AgCI) as a reference electrode (RE) and a chromium-gold (Cr/Au) as a seed layer on a glass substrate as a working electrode (WE). The Cr/Au seed layer was formed by an electron beam evaporator system. The electrolyte solution prepared consists of 3.2 mM Bi^{3+} and 7.2 mM $HTeO^{2+}$ in HNO_3. The electrolytes used for the deposition of nanocomposite films were prepared with a mixture of 0.75 g/L graphene nanoparticles and CNF (1 g/L). The mixing process underwent rigorous stirring conditions and was sonicated intermittently to ensure the appropriate result of the graphene/CNF nanoparticles dispersion and suspension in the electrolyte solution. An overview of the electrochemical deposition process is shown in Fig. 1.

Due to its highly hydrophilic nature, unmodified CNF tends to aggregate in organic solvents like N-methyl-2-pyrrolidone (NMP), leading to phase separation and poor film quality during electrodeposition. By introducing a cationic poly(diallyldimethylammonium chloride) (PDDA) envelopment, the surface charge of CNF was modified, enhancing its compatibility with the electrolyte and promoting better interaction with negatively charged graphene and Bi_2Te_3 particles [12,13]. This modification not only improved the dispersion stability of CNF but also contributed to a more homogeneous film formation. Prior to the deposition process, the CNF nanoparticles were coated with PDDA. The nanoparticles were mixed and sonicated in the diluted PDDA to ensure the polymeric molecules fully covered the surface of nanoparticle [14]. Then, the CNF nanoparticles in the PDDA solution went through the filtration process to filter the excessive PDDA solution. The electro-codeposition was performed in a potentiostatic periodic-reverse pulses deposition at room temperature. Meanwhile, the duty cycle ($T_{on}/(T_{on} + T_{off})$) was controlled at 33% for all depositions with rapid co-deposition occurred during 100 ms of T_{on} at applied potential –90 mV, E_{on}. The electrolyte was magnetically stirred at 100 rpm throughout the deposition process to preserve a uniform concentration of the graphene nanoparticles and the CNFs. The surface morphology and element composition were analyzed by scanning electron microscopy (SEM) and energy-dispersive X-ray spectroscopy (EDX).

RESULTS AND DISCUSSION

Cyclic voltammetry studies were performed using a potentiostat system of electrodeposition in the unstirred electrolyte solution. Cyclic voltammograms were obtained by electrochemical measurement system (NOVA Autolab) at a scan rate (10 mV/s) and the potential limits of the analysis have been fixed at -0.5 V to +1.0 V. Fig. 2 shows the cyclic voltammograms (CVs) of pristine Bi_2Te_3, graphene/Bi_2Te_3 and CNF-graphene/Bi_2Te_3. Cyclic voltammetry was performed on all samples to analyze the oxidation-reduction (redox) reaction at the working electrode and determine the optimal potential range for electrodeposition. Bi_2Te_3 formation occurs through the reduction of Bi^{3+} ions, concurrently with the co-deposition of Te derived from $HTeO_2^+$. The process involves the following possible half-reactions:

$$HTeO_2^+ + 3H^+ + 4e^- \rightarrow Te(s) + 2H_2O \quad (2)$$

$$3Te(s) + 2Bi^{3+} + 6e^- \rightarrow Bi_2Te_3(s) \quad (3)$$

The reduction peaks for pristine Bi_2Te_3, graphene/Bi_2Te_3 and CNF-graphene/Bi_2Te_3 were identified as R1, R2 and R3, respectively. A significant shift (negatively) in the reduction peak was observed for CNF (0.5)-graphene/Bi_2Te_3 compared to pristine Bi_2Te. This shift is attributed to the co-deposition of graphene and CNFs during Bi_2Te_3 reduction, which enhances electron transfer at the working electrode surface [1]. The reduction peak R2 was recorded at -60 mV, while R1 appeared at approximately -40 mV. A fixed potential of -90 mV (R3) was applied for all electrodepositions due to its role in promoting improved morphological growth of the deposited films in both CNF-graphene/Bi_2Te_3 and pristine Bi_2Te_3 [15].

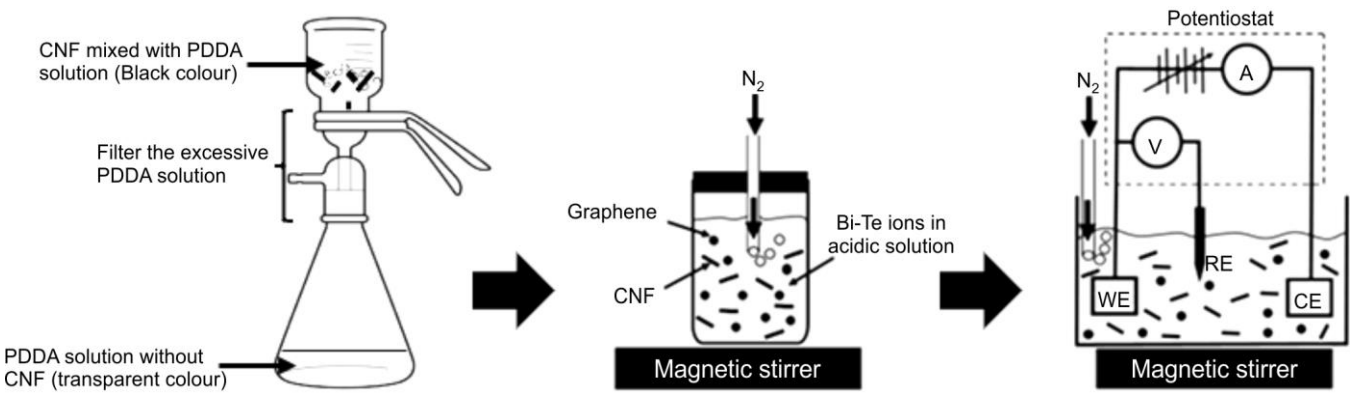

Fig. 1. Overview of film fabrication, including carbon nanofiber (CNF) and graphene

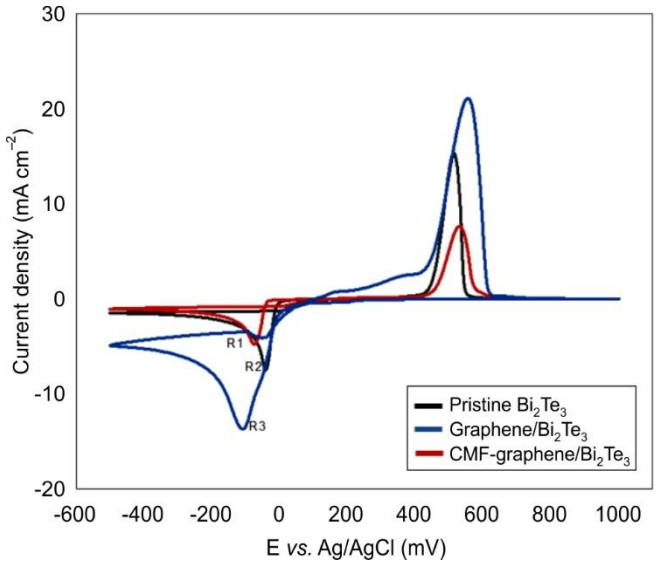

Fig. 2. Cyclic voltammograms of Bi^{3+} (3.2 mM) and $HTeO^{2+}$ (7.2 mM) in HNO_3 for pristine Bi_2Te_3, graphene/Bi_2Te_3, CNF-graphene/Bi_2Te_3

The use of higher cathodic potential during the electrodeposition of graphene-CNF/Bi_2Te_3 led to an increase in the reduction current. This indicates that a greater number of electrons were transferred during the diffusion of Bi/Te ions. As a result of accelerated crystal formation, the surface of the films grew more uneven and the colour changed from the usual grey to black. This effect was consistent with the findings of prior research on Bi_2Te_3, which were examined using potentiostatic electrochemical deposition methods [1,3].

The nanocomposite film of graphene-CNF/Bi_2Te_3, as shown in Fig. 3b, exhibits a uniform and smaller plate-like crystal structure compared to the pure Bi_2Te_3 films shown in Fig. 3a. By introducing CNF nanoparticles into Bi_2Te_3, the size of the plate-like crystals decreased, while maintaining a consistent Bi/Te atomic ratio up to a CNF content of 3.8 wt.% as presented in Table-1. Nevertheless, exceeding this amount of CNF content resulted in the composite material being too rigid right after the electrodeposition procedure.

The elemental composition of the graphene-CNF/Bi_2Te_3 nanocomposite films, as determined by EDX analysis, is summarized in Table-1. The maximum nanocomposite film weight is CNF-3.8 wt.%. Attempts were made to increase the ratio, however, the composite structure proved too stiff even after electrodeposition. This excessive stiffness contributed to the development of cracks, indicating that the structural integrity was compromised despite the modification efforts. The Bi/Te atomic ratio remained stable in the presence of varied amounts of CNF nanoparticles and the atomic percentage error, based on the stoichiometric ratio of Bi_2Te_3 phase, was consistently below 3.0%. The minimal deviation in the Bi_2Te_3 atomic ratio is important to ensure that variations in stoichiometry do not affect thermoelectric performance.

The inclusion of graphene into Bi_2Te_3 thermoelectric films greatly enhances their electrical conductivity, owing to the remarkable features exhibited by graphene as shown in Fig. 4. The highest electrical conductivity that has been achieved in this study was at 1956.18 S/cm from the 2.7 wt.% graphene-bismuth telluride deposited film. It was an increase of more than 200% compared to the pristine bismuth telluride

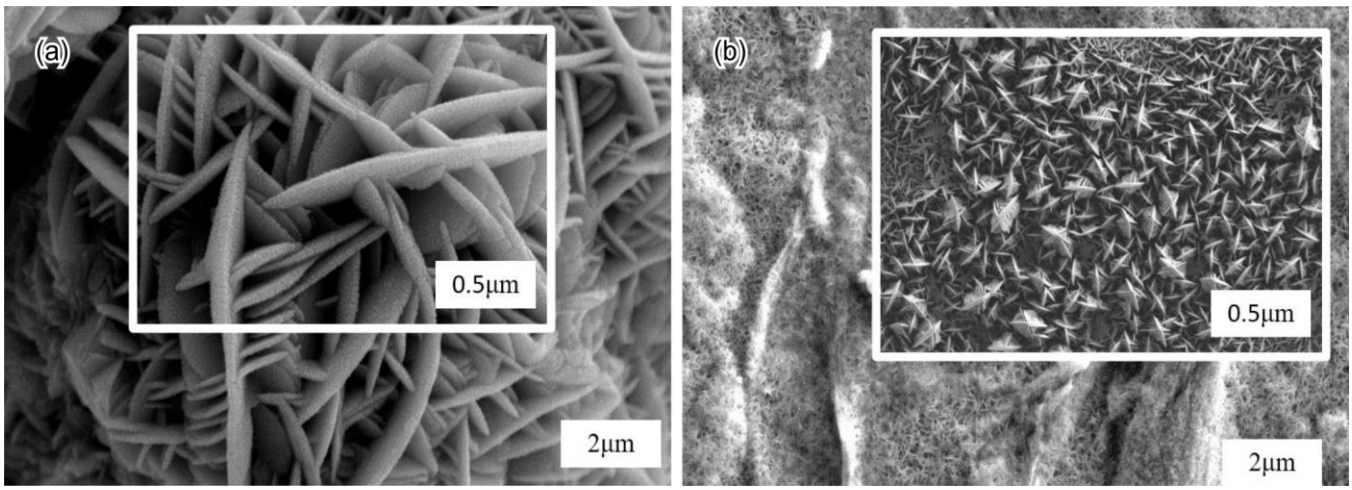

Fig. 3. SEM images of electrodeposited films of (a) Bi_2Te_3 and (b) graphene-CNF/Bi_2Te_3

TABLE-1
ELEMENT COMPOSITION OF ELECTRODEPOSITED FILMS FROM EDX ANALYSIS

Electrolyte	Graphene content in electrolyte (g/L)	CNFs content in electrolyte (g/L)	Electrodeposited film	Composition in the deposited film		
				Carbon (wt.%)	Bi:Te (at%)	Atomic % error due to Bi_2Te_3 phase ratio
I	0.00	0.0	Bi_2Te_3	0.0	38:62	± 2.0
II	0.25	0.0	Graphene/Bi_2Te_3-I	1.2	42:58	± 2.0
III	0.75	0.0	Graphene/Bi_2Te_3-II	1.6	37:63	± 3.0
IV	1.25	0.0	Graphene/Bi_2Te_3-III	2.7	42:58	± 2.0
V	0.75	1.0	Graphene-CNF/Bi_2Te_3	3.8	42:58	± 2.0

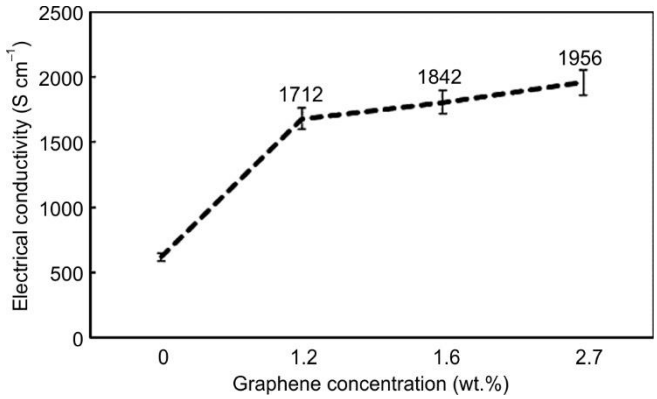

Fig. 4. Results of electrical conductivity of deposited graphene/Bi_2Te_3 films

at 618.65 S/cm. The high electrical conductivity of graphene generates the additional pathways for electron transport in the Bi_2Te_3 matrix, resulting in reduced resistance and improved overall electrical performance. Moreover, the 2D structure of graphene guarantees exceptional carrier mobility, enabling electrons to navigate the material with little dispersion, hence enhancing electrical conductivity. Moreover, graphene could function as a donor of carriers, thereby introducing additional charge carriers into the Bi_2Te_3 matrix and subsequently elevating the concentration of carriers. This, in turn, leads to an enhancement in electrical conductivity [16]. The combination of these features renders graphene a highly effective additive for enhancing the performance of Bi_2Te_3 thermoelectric films.

Fig. 5 demonstrates that the nanocomposite films exhibit higher hardness and Young's modulus compared to pure Bi_2Te_3 films, consistent with the previous findings [7,15] and other similar study [17]. The nanocomposite film with CNF inclusion indicates the highest micromechanical properties, with about 100% higher hardness and 34% higher Young's modulus than both pristine Bi_2Te_3 and graphene/Bi_2Te_3. The enhancement in micromechanical properties is attributed to strong interfacial adhesion between CNFs and the Bi_2Te_3 matrix, where CNFs function as reinforcing agents that effectively hinder localized plastic deformation. In addition, the van der Waals force that occurs at the interface between Bi_2Te_3 and CNFs results in a stable interfacial bonding that enables the transfer of load from the Bi_2Te_3 matrix to the CNFs [15,17]. Furthermore, the formation of smaller crystallite structures in the nanocomposites leads to the finer grain boundaries, which contributes to the observed increase in hardness and stiffness through the Hall-Petch effect.

Conclusion

This study presents a novel approach for fabricating bismuth telluride nanocomposite films incorporating hybrid nanoinclusions of graphene and cellulose nanofibers (CNFs) by electrochemical deposition. The successful fabrication of these nanocomposite films was achieved through the appropriate of electrolyte conditions and effective dispersion of graphene, resulting in a significant enhancement of electrical conductivity exceeding a 200% increase compared to the pristine Bi_2Te_3. The graphene-CNF/Bi_2Te_3 nanocomposite film exhibits a finer plate-like crystal morphology compared to the pristine Bi_2Te_3 film, accompanied by enhanced hardness and Young's modulus attributed to the reinforcing effect of CNFs. These results highlight the potential of graphene-CNF/Bi_2Te_3 hybrid nanocomposites as promising materials for advanced thermoelectric applications. Future research should focus on optimizing the concentration of graphene and CNFs, as well as investigating further overall thermoelectric performance.

ACKNOWLEDGEMENTS

The authors thank Universiti Teknikal Malaysia Melaka (UTeM) for all the support. This research is funded by Ministry of Higher Education (MOHE) of Malaysia through the Fundamental Research Grant Scheme (FRGS), No: FRGS/1/2023/TK08/UTeM/02/5.

CONFLICT OF INTEREST

The authors declare that there is no conflict of interests regarding the publication of this article.

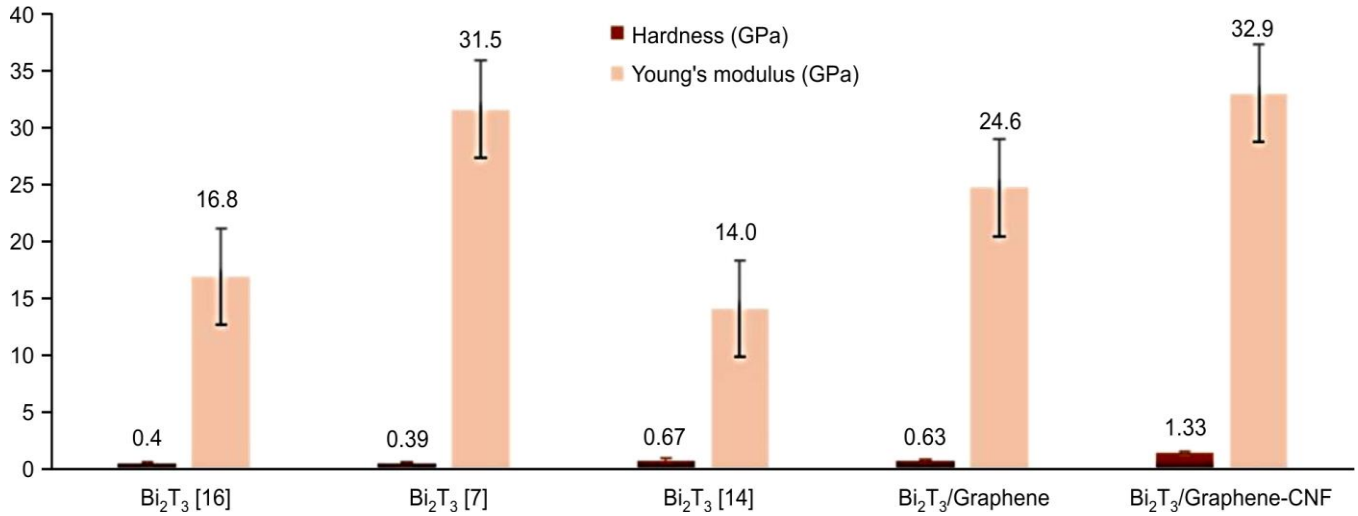

Fig. 5. Measured hardness and Young's modulus of Bi_2Te_3 and graphene-CNF/Bi_2Te_3

REFERENCES

1. D. Xu, Y. Wang, B. Xiong and T. Li, *Front. Mech. Eng*., **12**, 557 (2017); https://doi.org/10.1007/s11465-017-0441-2
2. A. Roncaglia and M. Ferri, *Sci. Adv. Mater.*, **3**, 401 (2011); https://doi.org/10.1166/sam.2011.1168
3. T.N. Huu, N.V. Toan and T. Ono, *Appl. Energy*, **210**, 467 (2018); https://doi.org/10.1016/j.apenergy.2017.05.005
4. N. Jaziri, A. Boughamoura, J.T. Müller, B. Mezghani, F. Tounsi and M.M. Ismail, *Energy Rep.*, **6**, 264 (2020); https://doi.org/10.1016/j.egyr.2019.12.011
5. M.K. Keshavarz, D. Vasilevskiy, R.A. Masut and S. Turenne, *Mater. Des.*, **103**, 114 (2016); https://doi.org/10.1016/j.matdes.2016.04.042
6. V. Rathi, K. Singh, S.K.P. Parmar, R.K. Brajpuriya and A. Kumar, *Org. Electron*., **133**, 107103 (2024); https://doi.org/10.1039/D4RA06184E
7. K.F. Samat, N.H. Trung and T. Ono, *Electrochim. Acta*, **312**, 62 (2019); https://doi.org/10.1016/j.electacta.2019.04.103
8. K. Ahmad and Z. Almutairi, *Mater. Today Commun*., **35**, 106228 (2023); https://doi.org/10.1016/j.mtcomm.2023.106228
9. A. Nour, H.M. Refaat, A. El-Dissouky and M.A. Soliman, *Ceram. Int.*, **49**, 26982 (2023); https://doi.org/10.1016/j.ceramint.2023.04.035
10. Q. Jiang, J. Yang, P. Hing and H. Ye, *Mater. Adv.*, **5**, 1038 (2020); https://doi.org/10.1039/d0ma00278j
11. X. Zhao, C. Zhao, Y. Jiang, X. Ji, F. Kong, T. Lin, H. Shao and W. Han, *J. Power Sources*, **479**, 229044 (2020); https://doi.org/10.1016/j.jpowsour.2020.229044
12. Z. Sun, Y. Liu, R. Wong, M. Yu, J. Li, M. Moran, M. Zhang, S. Dahariya, and C.-P. Wong, *Chem. Eng. J.*, **450**, 138299 (2022); https://doi.org/10.1016/j.cej.2022.138299
13. L. Dong, S. Ren, X. Zhang, Y. Yang, Q. Wu and T. Lei, *Carbohydr. Polym.*, **303**, 120463 (2022); https://doi.org/10.1016/j.carbpol.2022.120463
14. N.M. Nurazzi, M.R.M. Asyraf, A. Khalina, N. Abdullah, S. Ahmad, F.A. Sabaruddin, N.A. Kamarudin, A.M. Mahat, C.L. Lee, H.A. Aisyah, M.N.F. Norrrahim, R.A. Ilyas, M.M. Harussani, M.R. Ishak and S.M. Sapuan, *Polymers*, **13**, 1047 (2021); https://doi.org/10.3390/polym13071047
15. K.F. Samat, Y. Li, N. Van Toan, M.A. Azam and T. Ono, *J. Mater. Res.*, **37**, 3445 (2022); https://doi.org/10.1557/s43578-022-00508-2
16. B. Wu, Y. Guo, C. Hou, Q. Zhang, Y. Li and H. Wang, *Adv. Funct. Mater*., **29**, 1900304 (2019); https://doi.org/10.1002/adfm.201900304
17. Y. Song, I.J. Yoo, N.R. Heo, D.C. Lim, D. Lee, J.Y. Lee, K.H. Lee, K.H. Kim and J.H. Lim, *Curr. Appl. Phys*., **15**, 261 (2015); https://doi.org/10.1016/j.cap.2014.12.004